Journal of Advanced Marine Engineering and Technology, Vol. 47, No. 2, pp. 66~69, 2023
J. Advanced Marine Engineering and Technology (JAMET)
https://doi.org/10.5916/jamet.2023.47.2.66

ISSN 2234-7925 (Print)
ISSN 2765-4796 (Online)
Original Paper

Effect of precursor molecular structure while synthesizing hetero-carbon nanomaterials via solution plasma process

Koangyong Hyun†

(Received February 12, 2023 ; Revised March 27, 2023 ; Accepted April 11, 2023)

Abstract: Solution plasma processes (SPP) have recently attracted significant attention for the synthesis of heterocarbon nanomaterials (HCNs). However, to date, very few studies have reported the control of HCNs structures using SPP. Therefore, the factors affecting the structure of HCNs were investigated using a precursor with a similar molecular structure. In this study, powder X-ray diffraction and Raman spectroscopy results revealed that the nitrogen conjugation in the cyanopyrazine molecular structure could lead to facile crystalline carbon formation compared to the pyrazine precursor.

Keywords: Hetero-carbon nanomaterials, Solution plasma process, Precursor, Molecular structure, Crystalline carbon

1. Introduction

By doping carbon nanomaterials with heteroatoms, their chemical reactivities and electronic properties can be controlled by bandgap opening and modulation of the conducting types **[1]-[4]**. Nitrogen has been extensively investigated because of its similar size to carbon and the presence of five valence bonds with carbon atoms **[6]-[8]**.

Many studies have employed thermal treatment, among other methods, because it affects factors such as surface area, nitrogen content, nitrogen configuration, degree of graphitization, and conductivity **[5]-[7]**. Thermal treatment may improve the catalytic activity but reduce the total nitrogen content, thereby reducing the surface density of the catalytic sites. This limits their catalytic activity.

Recently, the solution plasma process (SPP), known as non-equilibrium cold plasma at atmospheric pressure and room temperature **[8]**, has been used to synthesize heterocarbon nanomaterials (HCNs) **[9]**. Heterocarbons with multiple catalytic sites can be obtained by direct polymerization of liquid materials, and designing ideal catalysts using SPP may be possible. To date, studies on nitrogen content and doping position control have been conducted using SPP **[10]**.

However, very few studies have reported controlling the structures of heterocarbons using SPP. Moreover, precise control of the carbon structure during the production of carbon nanosheets has not yet been analyzed **[11]-[13]**.

Therefore, in this study, the factors affecting the structure of HCNs were investigated using precursors with similar molecular structures. Differences were observed in the carbon structures under the same SPP conditions. Based on these differences, the carbon structure could be controlled using SPP in the future.

2. Experimental procedure

The experimental setup for SPP consisted of two tungsten electrodes connected to a bipolar pulsed power supply (Kurita, Japan) in a glass reactor **[10]**. The reactor was filled with 100 mL of an aqueous precursor as the carbon or nitrogen source for the synthesis of HCNs.

Pyrazine (PY; $C_4H_4N_2$, 99.0%) and cyanopyrazine (CY; $C_5H_3N_3$, 99.0%) were purchased from Tokyo Chemical Industry and used as precursors because of their similar molecular structures. Further, the influence of the precursor on the shape of the obtained carbon nanomaterials was investigated. HCNs prepared from PY and CY were denoted as HCNs–PY and HCNs–CY, respectively.

A plasma discharge with a 1.0 μs repetition pulse width and 100 kHz repletion frequency was generated in the precursors at atmospheric pressure and room temperature. The solution in the reaction vessel was then stirred at 60 °C. After discharge, the black carbon particles were separated using vacuum filtration. The as-synthesized carbon nanomaterials were dried in an oven at 200 °C for 1 h.

† Corresponding Author (ORCID: https://orcid.org/0000-0002-6894-7001): Assistant Professor, Division of Naval Officer Science, Mokpo National Maritime University, 91, Haeyangdaehak-ro, Mokpo-si, Jeollanam-do 58628, Korea, E-mail: kyhyun@mmu.ac.kr, Tel: +82-61-240-7124

This is an Open Access article distributed under the terms of the Creative Commons Attribution Non-Commercial License (http://creativecommons.org/licenses/by-nc/3.0), which permits unrestricted non-commercial use, distribution, and reproduction in any medium, provided the original work is properly cited.

Copyright ⓒ The Korean Society of Marine Engineering

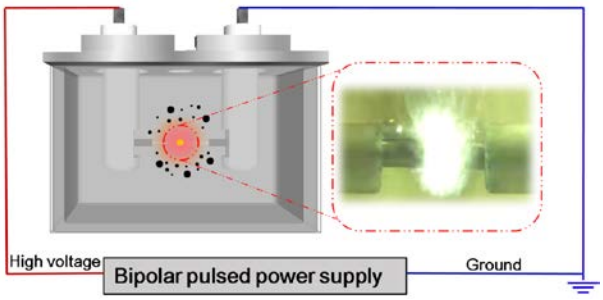

Figure 1: Illustration of solution plasma process

Transmission electron microscopy (TEM) images were obtained using a JEOL-2500SE microscope at an acceleration voltage of 200 kV. Powder X-ray diffraction (XRD) was used to examine the crystal structure using an X-ray diffractometer

(Rigaku Smartlab) with Cu Kα radiation (λ = 0.154 nm). Raman spectra were obtained using a JASCO NRS-100 spectrometer at an excitation wavelength of 532.5 nm. Elemental analyses of C, H, and N were performed using an elemental analyzer (Perkin Elmer 2400 Series).

3. Results and discussion

The morphologies of HCNs–PY and HCNs–CY are shown in **Figure 2**. All HCNs–PY and HCNs–CY formed agglomerates of uniform nanosized carbon particles with a three-dimensional interconnected structure. HCNs–PY exhibited a ball-like shape with diameters in the range of 20–30 nm. The sizes of HCNs–CY, which had irregular shapes, were in the range of 30–80 nm and were larger than those of HCNs–PY. In the high-resolution TEM image shown in **Figure 2(d)**, long-range ordered graphitized carbons with lattice fringes corresponding to the (002) basal plane of turbostratic carbon were observed. However, high-resolution TEM images of HCNs–PY showed clear differences in their structures, such as an amorphous structure without any clear shape **[14]**. These results indicate that the morphology of HCNs prepared by SPP strongly depends on the precursors used.

Figure 3 shows the powder XRD patterns of HCNs–PY and HCNs–CY. The diffraction peaks of HCNs–PY exhibited a broad peak at 24.3° and a small peak at 43.3°, corresponding to the (002) and (100)/(101) graphite planes in turbostratic carbon, respectively **[15][19][20]**. The XRD patterns of HCNs–CY exhibited similar broad peaks at approximately 43.5°. The peak corresponding to the (002) plane was sharper and shifted toward the higher 2θ values (25.3°) compared to that of HCNs–PY, which indicates a decrease in the sp^2 layer spacing **[19][20]**. The results reveal that the degree of graphitic order in HCNs–CY was much higher than HCNs–PY **[20]**. This suggests that the precursor

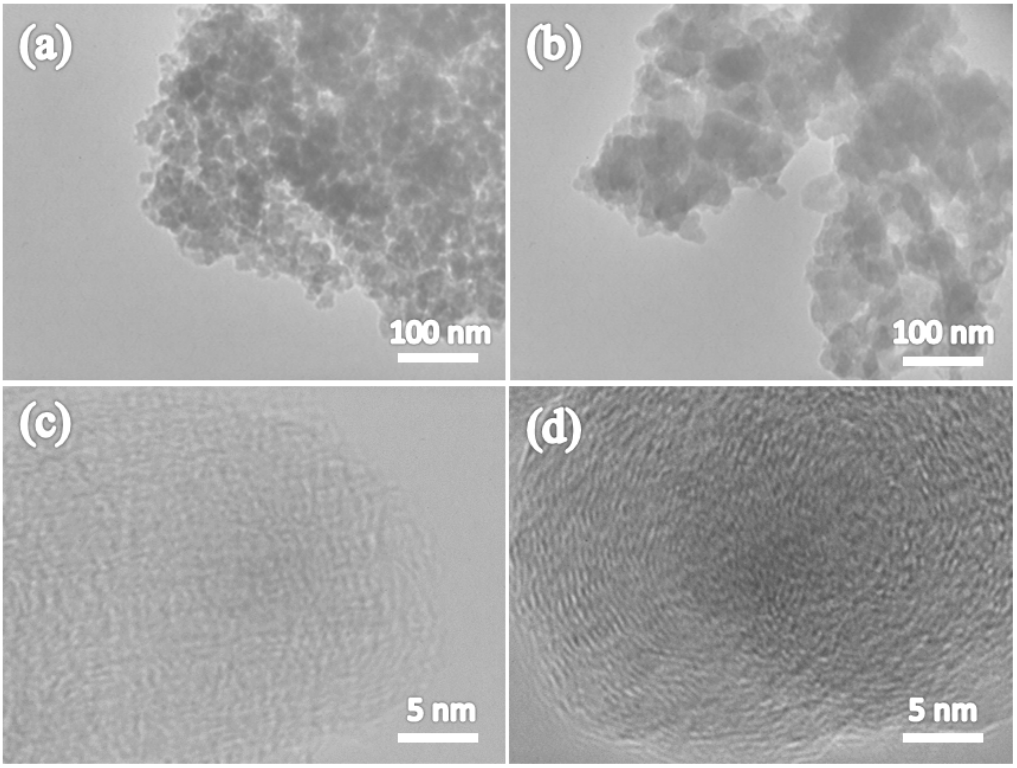

Figure 2: TEM images of (a, and c) HCNs–PY and (b, and d) HCNs–CY

molecule structure determines the structural properties of HCNs prepared using SPP. For reference, weak-intensity peaks corresponding to tungsten carbide (WC_{1-x}) were observed at 36.8° (111) and 42.5° (200) for both HCNs-PY and HCNs-CY **[18]**.

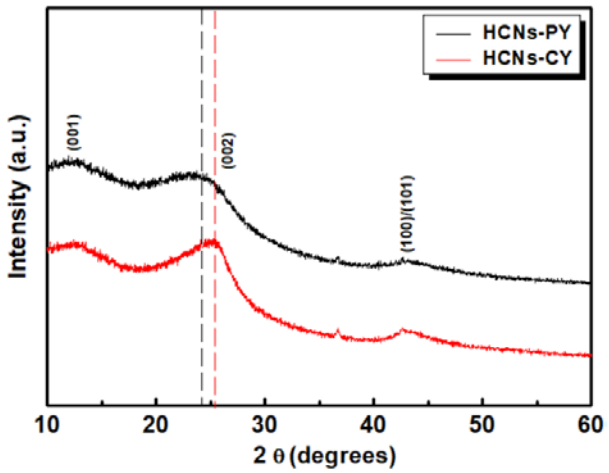

Figure 3: XRD patterns of HCNs–PY and HCNs–CY

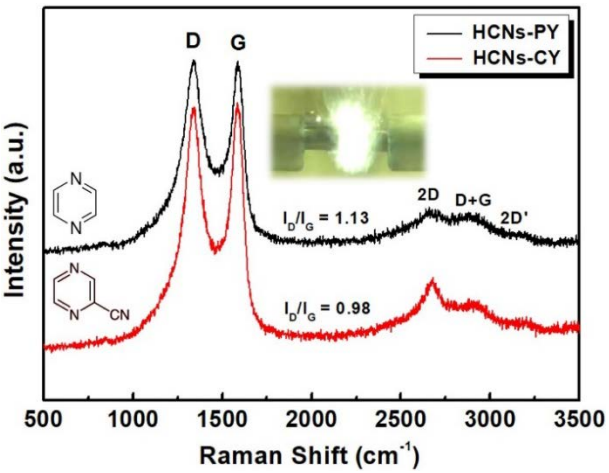

Figure 4: Raman spectra of HCNs–PY and HCNs–CY

Figure 4 shows the typical Raman spectra of HCNs–PY and HCNs–CY. The relative intensity ratio of the D- and G-bands (I_D/I_G) indicates the graphitization degree or defect density of the carbon nanomaterials **[16]**. This ratio was used to calculate the in-plane crystallite size (L_a) using the following equation:

$$L_a = (2.4 \times 10^{-10})\lambda_l^4 (I_D/I_G)^{-1} \quad (1)$$

where λ_l (nm) is the wavelength of the laser line **[17]**. The corresponding La values of the carbon nanomaterials are 17.1 and 19.7 for HCNs–PY and HCNs–CY, respectively. Furthermore, a 2D band in the range of 2600–2800 cm^{-1}, corresponding to the presence of a highly ordered carbon lattice, was also observed. Notably, a significant difference was observed in the 2D band intensities in the Raman spectra of HCNs–PY and HCNs–CY. The intensity of the 2D band of HCNs–CY was higher than that of HCNs–PY. Therefore, the CN conjugation in the CY molecular structure could lead to facile crystalline carbon formation. The successful incorporation of nitrogen within the carbon was confirmed by elemental analysis. HCNs–PY and HCNs–CY contained 14.98 and 16.11 wt.% nitrogen, respectively.

4. Conclusions

Very few studies have focused on controlling the structures of heterocarbons using the SPP. Therefore, the factors affecting the structure of HCNs were investigated using a precursor with a similar molecular structure. PY and CY were used as precursors to investigate the influence of the nature of the precursors on the shape of the obtained carbon nanomaterials. The morphologies of HCNs prepared using SPP strongly depend on the precursors used. Moreover, the influence of the precursor molecular structure determines the structural properties of HCNs prepared through SPP. The XRD and Raman spectra indicated that CN conjugation in the CY molecular structure led to facile crystalline carbon formation. Finally, under the same SPP conditions, there were differences in the carbon structures; based on these differences, the carbon structure can be controlled using SPP in the future.

Acknowledgement

This work was supported by the National Research Foundation of Korea(NRF) grant funded by the Korea goverment(MSIT) (No. 2019R1G1A1007887).

Author Contributions

Conceptualization, K. Hyun; Methodology, K. Hyun; Software, K. Hyun; Validation, K. Hyun; Formal Analysis, K. Hyun; Investigation, K. Hyun; Resources, K. Hyun; Data Curation, K. Hyun; Writing—Original Draft Preparation, K. Hyun; Writing—Review & Editing, K. Hyun; Visualization, K. Hyun; Supervision, K. Hyun; Project Administration, K. Hyun; Funding Acquisition, K. Hyun.

References

[1] H. Peng, G. Ma, K. Sun, J. Mu, and Z. Lei, “One-step preparation of ultrathin nitrogen-doped carbon nanosheets with

ultrahigh pore volume for high-performance supercapacitors," Journal Materials Chemistry A, vol. 2, no. 41, pp. 17297-17301, 2014.

[2] V. V. Strelko, V. S. Kuts, and P. A. Thrower, "On the mechanism of possible influence of heteroatoms of nitrogen, boron and phosphorus in a carbon matrix on the catalytic activity of carbons in electron transfer reactions," Carbon, vol. 38, no. 10, pp. 1499-1503, 2000.

[3] D. Wei, Y. Liu, Y. Wang, H. Zhang, L. Huang, and G. Yu, "Synthesis of N-doped graphene by chemical vapor deposition and its electrical properties," Nano Letters, vol. 9, no. 5, pp. 1752-1758, 2009.

[4] L. S. Panchokarla, K. S. Subrahmanyam, S. K. Saha, A. Govindaraj, H. R. Krishnamurthy, U. V. Waghmare, and C. N. R. Rao, "Synthesis, structure, and properties of boron- and nitrogen-doped graphene," Advanced Materials, vol. 21, no. 46, pp. 4726-4730, 2009.

[5] Q. Kuang, S. Y. Xie, Z. Y. Jiang, X. H. Zhang, Z. X. Xie, R. B. Huang, and L. S. Zheng, "Low temperature solvothermal synthesis of crumpled carbon nanosheets," Carbon, vol. 42, no. 8-9, pp. 1737-1741, 2004.

[6] W. Wang, S. Chakrabarti, Z. Chen, Z. Yan, M. O. Tade, J. Zou, and Q. Li, "A novel bottom-up solvothermal synthesis of carbon nanosheets," Journal Materials Chemistry A, vol. 2, no. 7, pp. 2390-2396, 2014.

[7] C. Zhang, L. Fu, N. Liu, M. Liu, Y. Wang, and Z. Liu, "Synthesis of Nitrogen-doped graphene using embedded carbon and nitrogen Sources", Advanced Materials, vol. 23, no. 8, pp. 1020-1024, 2011.

[8] O. Takai, "Solution plasma processing (SPP)," Pure and Applied Chemistry, vol. 80, no. 9, pp. 2003-2011, 2008.

[9] G. Panomsuwan, N. Saito, and T. Ishizaki, "Nitrogen-doped carbon nanoparticle–carbon nanofiber composite as an efficient metal-free cathode catalyst for oxygen reduction reaction," ACS Applied Materials & Interfaces, vol. 8, no. 11, pp. 6962-6971, 2016.

[10] O. L. Li, H. Lee, and T. Ishizaki, "Recent progress in solution plasma-synthesized-carbon-supported catalysts or energy conversion systems," Japanese Journal of Applied Physics, vol. 57, no. 1, 0102A2, 2018.

[11] K. Hyun, T. Ueno, O. L. Li, and N. Saito, "Synthesis of heteroatom-carbon nanosheets by solution plasma processing using *N*-methyl-2-pyrrolidone as precursor," RSC Advances, vol. 6, no. 9, pp. 6990-6996, 2016.

[12] K. Hyun, T. Ueno, G. Panomsuwan, O. L. Li, and N. Saito, "Heterocarbon nanosheets incorporating iron phthalocyanine for oxygen reduction reaction in both alkaline and acidic media," Physical Chemistry Chemical Physics, vol. 18, no. 16, pp. 10856-10863, 2016.

[13] K. Hyun and N. Saito, "The solution plasma process for heteroatom-carbon nanosheets: the role of precursors," Scientific Reports, vol. 7, p. 3825, 2017.

[14] A. G. Ramírez, T. Itoh, and R. Sinclair, "Crystallization of amorphous carbon thin films in the presence of magnetic media," Journal of Applied Physics, vol. 85, p. 1508, 1999.

[15] G. Panomsuwan, S. Chiba, Y. Kaneko, N. Saito, and T. Ishizaki, "In situ solution plasma synthesis of nitrogen-doped carbon nanoparticles as metal-free electrocatalysts for the oxygen reduction reaction," Journal of Materials Chemistry A, vol. 2, no. 43, pp. 18677-18686, 2014.

[16] N. Li, Z. Wang, K. Zhao, Z. Shi, Z. Gu, and S. Xu, "Large scale synthesis of N-doped multi-layered graphene sheets by simple arc-discharge method," Carbon, vol. 48, no. 1, pp. 255-259, 2010.

[17] L. G. Cancado, K. Takai. T. Enoki, M. Endo, Y. A. Kim, H. Mizusaki, A. Jorio, L. N. Coelho, R. M-. Paniago, and M. A. Pimenta, "General equation for the determination of the crystallite size La of nanographite by Raman spectroscopy," Applied Physics Letters, vol. 88, 163106, 2006.

[18] K. Hyun, T. Ueno, and N. Saito, "Synthesis of nitrogen-containing carbon by solution plasma in aniline with high-repetition frequency discharges," Japanese Journal of Applied Physics, vol. 55, no. 15, 01AE18, 2016.

[19] D. Bhattachariya, H. -Y. Park, M. -S. Kim, H. -S. Choi, S. N. Inamdar, and J. -S. Yu, "Nitrogen-doped carbon nanoparticles by flame synthesis as anode material for rechargeable lithium-ion batteries," Langmuir, vol. 30, no. 1, pp. 318-324, 2014.

[20] Z. Q. Li, C. J. Lu, Z. P. Xia, Y. Zhou, and Z. Luo, "X-ray diffraction patterns of graphite and turbostratic carbon," Carbon, vol. 45, no. 8, pp. 1686-1695, 2007.